Макрогетероциклы
http://macroheterocycles.isuct.ru

DOI: 10.6060/mhc200285k

Influence of Electron−Donating Substituents on the Stability of Sandwich−Type Complexes of Crown−Containing Anthraquinoneimines

Aleksandra A. Kudrevatykh,[a@] Timofey P. Martyanov,[b] Evgeny N. Ushakov,[b] Alexander V. Chernyak,[b,c] and Lubov S. Klimenko[a]

[a] *Yugra State University, 628012 Khanty-Mansiysk, Russia*
[b] *Institute of Problems of Chemical Physics RAS, 142432 Chernogolovka, Russia*
[c] *Science Center in Chernogolovka RAS, 142432 Chernogolovka, Russia*
[@] *Corresponding author E-mail: Alexandra.korolkova@mail.ru*

New 4'-(1-hydroxy-9,10-anthraquinone-9-imino)benzo-15-crown-5 ether derivatives containing a phenoxy group at the position 2 or 4 of the anthraquinone moiety were synthesized photochemically. The complexing properties of these compounds in acetonitrile were studied by spectrophotometry. Two analogous derivatives, one of which has no substituents in positions 2 and 4, and the other one contains benzoylamino group in position 2, were used in this study as the reference ligands. It was demonstrated that the synthesized dyes are capable of binding the Sr^{2+} and Ba^{2+} ions to form 2:1 (ligand–metal) sandwich-type complexes that exhibit higher stability constants than the corresponding 1:1 complexes. The molecular structures of the biligand complexes with Ba^{2+} in solution were studied by dispersion-corrected density functional theory calculations.

Keywords: π-Stacking, sandwich complexes, crown compounds, anthraquinones, tautomerism.

Влияние электронодонорных заместителей на устойчивость сэндвичевых комплексов краунсодержащих антрахнониминов

А. А. Кудреватых,[a@] Т. П. Мартьянов,[b] Е. Н. Ушаков,[b] А. В. Черняк,[b,c]
Л. С. Клименко[a]

[a] *Югорский государственный университет, 628012 Ханты-Мансийск, Россия*
[b] *Институт проблем химической физики РАН, 142432 Черноголовка, Россия*
[c] *Научный центр в Черноголовке РАН, 142432 Черноголовка, Россия*
[@] *E-mail: Alexandra.korolkova@mail.ru*

Фотохимическим путем синтезированы новые производные 4'-(1-гидрокси-9,10-антрахинон-9-имино)бензо-15-краун-5-эфира, содержащие феноксигруппу в положении 2 или 4 антрахинонового фрагмента. С помощью спектрофотометрии исследованы комплексообразующие свойства этих соединений в ацетонитриле. В качестве референсных лигандов использовали два аналогичных производных, одно из которых не имеет заместителей в положениях 2 и 4, а другое содержит бензоиламиногруппу в положении 2. Показано, что синтезированные красители способны связывать ионы Sr^{2+} и Ba^{2+} с образованием сэндвичевых комплексов 2:1 (лиганд–металл), которые имеют более высокие константы устойчивости, чем соответствующие комплексы 1:1. Молекулярные структуры билигандных комплексов с Ba^{2+} в растворе были изучены с помощью теории функционала плотности с поправкой на дисперсионные силы.

Ключевые слова: π-Стэкинг, сэндвичевые комплексы, краун-соединения, антрахиноны, таутомеризм.

Introduction

Intermolecular interactions involving aromatic rings are key processes in both chemical and biological recognition.[1] Arene–arene interactions, such as π-stacking, play an important role in the structure of DNA and RNA, as well as in the folding[2,3] and thermal stability of proteins.[4] However, the weakness and poor directionality of these interactions hinder the development of a general (structural and energetic) model for their description.[5,6] New information on the relationship between the molecular structure and the strength of arene–arene interactions is relevant and important and can be used in the design of materials for bioengineering,[7] organic molecular electronics,[8] and spintronics.[9]

It is known that crown ethers are able to form 2:1 (ligand–metal) sandwich-type complexes with metal cations that are larger in diameter than the crown ether cavity.[10,11] This feature has been used to create new "smart" materials, such as ion-responsive membranes with functional gates driven by host–guest molecular recognition,[12,13] ion-imprinted hydrogels,[14] supramolecular gels with high mechanical strength,[15] polymers with ion-dependent hydrophobic properties,[16] ion-responsive photonic devices,[17–19] antibiotics and antifungal remedies,[20] crown ether-modified nanoparticles capable of changing their spectral properties owing to the formation of sandwich complexes.[21,22] These materials have promising applications in self-healing technology, targeted drug delivery systems, and optical sensors for the detection of metal cations. The formation of sandwich complexes can significantly affect the ion transport through liquid membranes doped with crown ethers,[12,13] which is important to take into account when designing simple artificial models of biological systems.

Despite the variety of existing molecular devices, the action of which is based on the formation of host–guest sandwich complexes, the influence of interactions between peripheral units of the host molecules on the complex stability remains poorly understood.[23,24] Previously, we have reported that 2:1 (ligand–metal) sandwich complexes formed by benzo-15-crown-5 derivatives containing an anthraquinoneimine chromophore can exhibit higher stability constants than the corresponding 1:1 complexes owing to interchromophoric interactions.[25,26] In particular, it was found that the stability constant of the 2:1 complex of dye **1c** with Ba^{2+} in MeCN is twice higher than that of the corresponding 1:1 complex. According to quantum chemical calculations, the two chromophores in complex $(\mathbf{1c})_2 \cdot Ba^{2+}$ adopt an *anti* orientation relative to each other, in which there are stacking contacts between the aromatic rings **C** and between the benzene rings **D**. The presence of a benzoylamino group in the 2 position of the anthraquinone moiety of dye **1c** (compound **1d**) led to a further increase in the relative stability of the 2:1 complex.

It is known that the introduction of a substituent of any nature into one of the rings in the π-stacked benzene dimer leads to an increase in the intermolecular interaction energy.[5,27,28] In the case of acceptor substituents, the higher the electron-withdrawing ability of the substituent is the stronger the interaction energy. As concerns donor substituents, there are discrepancies on how the interaction energy depends on the electron-donating ability of the substituent.[5,28] Previously, we have shown that the *para*-substitution of the benzoyl ring in dye **1d** with a nitro group provides an almost twofold increase in the stability constants of sandwich complexes with Sr^{2+} and Ba^{2+}.[29] In order to study the effect of electron-donating substituents on the stability of the sandwich complexes formed by crown-containing anthraquinoneimines, we synthesized two phenoxy derivatives of dye **1c**, namely, compounds **1a**,**b**.

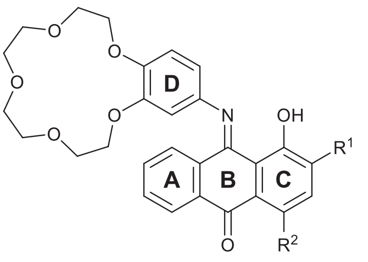

1a: R^1 = –OPh; R^2 = H
1b: R^1 = H; R^2 = –OPh
1c: R^1 = R^2 = H
1d: R^1 = –NHCOPh; R^2 = H

Experimental

General Remarks

Column chromatography was carried out on Silicagel 60 (0.063–0.100 mm). TLC analysis was performed using Silufol UV-254 plates. Host–guest complexation studies were conducted in acetonitrile of special purity grade (water content < 0.03 %, v/v). In other cases, solvents of high and very high purity grades were used. $Mg(ClO_4)_2$, $Ca(ClO_4)_2$, $Sr(ClO_4)_2$, and $Ba(ClO_4)_2$ were dried *in vacuo* at 230 °C.

^1H and ^{13}C NMR spectra were measured on a Bruker AVANCE III 500 spectrometer. The solvent (MeCN-d_3 or $CDCl_3$) was used as the internal reference.[30] Absorption spectra were recorded on a Specord M40 spectrophotometer. Elemental analysis was carried out using a Vario MICRO Cube analyzer. IR spectra were recorded on a Bruker Alpha FTIR spectrometer in an ATR unit.

Synthesis

Synthesis of 2-amino-1-chloroanthraquinone (3). Compound **3** was prepared using the general procedure described in literature.[31] A solution of SO_2Cl_2 (1.14 mL, 0.014 mol) in chlorobenzene (15 mL) was slowly added dropwise to a mixture of 2-aminoanthraquinone (2.23 g, 0.01 mol), DMF (0.2 mL), and chlorobenzene (30 mL); then the reaction mixture was stirred at room temperature for 1 h. The addition of hexane (30 mL) at the end of the reaction (monitoring by TLC) led to the formation of a precipitate, which was filtered off, washed with hexane (10 mL), and recrystallized from a mixture of ethanol and toluene (1:1, v/v); the filtered solid was dried at 50 °C for 5 hours. Yield: 93 %; orange powder.

Synthesis of 1,2-dichloroanthraquinone (4a). 2-Amino-1-chloroanthraquinone (**3**, 1.7 g, 6.6 mmol) was dissolved in glacial acetic acid (30 mL) with heating. After the solution was cooled to room temperature, 36 % hydrochloric acid (1.8 mL) was added. The resulting suspension was cooled in an ice bath to 0 °C, and then a solution of KNO_2 (0.65 g, 7.59 mmol) in water (2 mL) was slowly added dropwise with stirring. The subsequent steps were the addition of CuCl (0.8 g, 8.1 mmol) dissolved in a mixture of 36 % hydrochloric acid (2.3 mL) and water (25 mL), stirring for 30 minutes at 0 °C, the addition of water (20 mL), heating for 2 hours at 100 °C, cooling to room temperature, filtering off the resulting precipitate, and washing it first with a 40 % KOH solution and then with water. The solid residue was dried and then chromatographed on a column with SiO_2 (40–63 μm) using toluene as the eluent. After the yellow fraction (target product) was isolated, the solution was evaporated under reduced pressure, and the solid residue was dried at 50 °C for 3 h. Yield: 79 %; yellow powder. ^{1}H NMR (500 MHz, $CDCl_3$) δ_H ppm: 8.27–8.31 (m, 1H, H-8), 8.22–8.26 (m, 2H, H-4,5), 7.85–7.90 (m, 1H, H-3), 7.77–7.85 (m, 2H, H-6,7).

*Synthesis of 1,2- and 1,4-diphenoxyanthraquinones (**5a,b**).* Compound **4a** or **4b** (0.35 g, 1 mmol) and C_6H_5ONa (0.12 g, 1 mmol) were dissolved in a mixture of toluene (80 mL) and DMSO (20 mL). The solution was stirred at room temperature for 10 h until the starting dichloroanthraquinone was completely consumed (monitoring by TLC). After the addition of water (100 mL) and a few drops of 36 % hydrochloric acid, the reaction mixture was extracted with toluene (three times by 50 mL). The extract was dried with calcined $MgSO_4$, evaporated to 10–15 mL, and then chromatographed on a column with SiO_2 (40–63 μm) using toluene as the eluent. The main yellow fraction with the target compound was isolated and evaporated to 5–10 mL. The subsequent addition of hexane led to the formation of a crystalline precipitate, which was filtered off, washed with hexane, dried at room temperature, and then recrystallized from a mixture of ethanol and benzene (4:1, v/v).

*1,2-Diphenoxyanthraquinone (**5a**).* Yield: 81 %; yellow powder. M.p.: 197–198 °C. Elemental analysis calcd (%) for $C_{26}H_{16}O_4$: C 79.58, H 4.11; found: C 79.74, H 4.15. IR ν_{max} cm^{-1}: 3069, 3036 (CH_{ar}), 1670 (C=O), 1591, 1564 (C=C_{ar}). ^{1}H NMR (500 MHz, $CDCl_3$) δ_H ppm: 8.17–8.30 (m, 3H, H-4,5,8), 7.71–7.81 (m, 2H, H-6,7), 7.35 (m, 2H, H-3′,5′), 7.24–7.41 (m, 3H, H-3,3″,5″), 7.18 (t, 1H, J = 7.4 Hz, H-4’), 7.02 (t, 1H, J = 7.4 Hz, H-4’’), 7.24–7.41 (m, 4H, H-2’,6’,2’’,6’’).

*1,4-Diphenoxyanthraquinone (**5b**).* Yield: 75 %; yellow powder. M.p.: 125–127 °C. The spectral data and elemental analysis for this compound were reported previously.[32]

*Synthesis of crown compounds **1a,b** (general procedure).* Compound **5a** or **5b** (0.29 g, 0.5 mmol) and 4′-aminobenzo-15-crown-5 (0.17 g, 0.6 mmol) were dissolved in benzene (150 mL). The solution was exposed to sunlight for 5–6 h. At the end of the photoreaction (monitoring by TLC), the solution was evaporated to 10–15 mL and then chromatographed on a column with SiO_2 using gradient elution (the eluent polarity was increased by adding ethanol to benzene). The main brick-red fraction containing the target product was isolated and evaporated to 5–10 mL. The subsequent addition of hexane led to the formation of a crystalline precipitate, which was filtered off, washed with hexane, dried at room temperature, and then recrystallized from a mixture of ethanol and benzene.

*4′-(1-Hydroxy-2-phenoxy-9,10-anthraquinone-9-imino) benzo-15-crown-5 (**1a**).* Yield: 70 %; brick-red powder. M.p.: 185–187 °C. Elemental analysis calcd (%) for $C_{34}H_{31}NO_8$: C 70.21, H 5.37, N 2.41; found: C 70.44, H 5.61, N 2.38. IR ν_{max} cm^{-1}: 3435 (OH), 3062 (CH_{ar}), 2913, 2862 (CH_{alk}), 1655 (C=O), 1618 (C=N), 1585 (C=C_{ar}). ^{1}H NMR (500 MHz, $CDCl_3$) δ_H ppm: 15.52 (s, 1H, OH), 8.19 (dd, 1H, J = 7.8 and 1.1 Hz, H-5), 7.66–7.75 (m, 2H, H-4,6), 7.50–7.56 (m, 1H, H-7), 7.45–7.50 (m, 1H, H-8), 7.36–7.41 (m, 2H, H-3″,5″), 7.35 (d, 1H, J = 8.4 Hz, H-3), 7.10–7.16 (m, 1H, H-4″), 6.98–7.05 (m, 3H, H-5’,2’’,6’’), 6.89 (d, 1H, J = 2.4 Hz, H-2’), 6.70 (dd, 1H, J = 8.4 and 2.3 Hz, H-6’), 4.04–4.12 (m, 2H, H-α),3.88–4.01 (m, 2H, H-α′), 3.75–3.82 (m, 2H, H-β), 3.67–3.73 (m, 2H, H-β′), 3.57–3.66 (m, 8H, H-γ,γ′,δ,δ′). ^{13}C NMR (500 MHz, $CDCl_3$) δ_C ppm: 181.99 (C-10), 159.53 (C-9), 156.77 (C-2), 153.22 (C-1), 149.61 (C-4′), 149.10 (C-1″), 146.85 (C-3′), 140.26 (C-3′), 132.41 (C-6), 133.52 (C-11), 132.23 (C-7), 129.97 (C-8), 129.67 (C-3″,5″), 128.84 (C-12), 128.33 (C-14), 127.57 (C-5), 127.28 (C-4″), 123.42 (C-3), 119.00 (C-13), 117.26 (C-2″,6″), 114.54 (C-5′), 112.69 (C-6′), 106.85 (C-2′), 70.52 (C-δ), 70.44 (C-δ′), 69.73 (C-γ), 69.66 (C-γ′), 68.83 (C-β), 68.60 (C-α), 69.57 (C-β′), 68.38 (C-α′).

*4′-(1-Hydroxy-4-phenoxy-9,10-anthraquinone-9-imino) benzo-15-crown-5 (**1b**).* Yield: 78 %; brick-red powder. M.p.: 191–193 °C. Elemental analysis calcd (%) for $C_{34}H_{31}NO_8$: C 70.21, H 5.37, N 2.41; found: C 70.61, H 5.58, N 2.31. IR ν_{max} cm^{-1}: 3436 (OH), 3062 (CH_{ar}), 2913, 2862 (CH_{alk}), 1675 (C=O), 1612 (C=N), 1591, 1561 (C=C_{ar}). ^{1}H NMR (500 MHz, $CDCl_3$) δ_H ppm: 14.97 (s, 1H, OH), 7.94 (dd, 1H, J = 7.8 and 0.9 Hz, H-5), 7.59–7.64 (m, 1H, H-6), 7.44–7.50 (m, 1H, H-7), 7.27–7.38 (m, 5H, H-2,3,3’’,5’’,8), 7.02–7.07 (m, 1H, H-4’’), 7.00 (d, 1H, J = 8.4 Hz, H-5’), 6.87–6.91 (m, 2H, H-2’’,6’’), 6.86 (d, 1H, J = 2.3 Hz, 2’), 6.69 (dd, 1H, J = 8.4 and 2.3 Hz, 6’), 4.04–4.11 (m, 2H, H-α), 3.89–4.98 (m, 2H, H-α′), 3.75–3.82 (m, 2H, H-β), 3.67–3.72 (m, 2H, H-β′), 3.57–3.66 (m, 8H, H-γ,γ′,δ,δ′). ^{13}C NMR (500 MHz, $CDCl_3$) δ_C ppm: 181.91 (C-10), 159.32 (C-9), 158.44 (C-4), 157.38 (C-1), 149.55 (C-3′), 146.72 (C-4′), 146.39 (C-1″), 140.81 (C-1′), 134.98 (C-11), 132.09 (C-6), 131.68 (C-7), 129.68 (C-8), 128.97 (C-12), 128,45 (C-2), 128.36 (C-3″,5″), 126.77 (C-5), 124.90 (C-3), 123.69 (C-14), 122.04 (C-4″), 117.78 (C-13), 116.30 (C-2″,6″), 114.55 (C-5′), 112.83 (C-6′), 106.92 (C-2′), 70.52 (C-δ), 70.44 (C-δ′), 69.74 (C-γ), 69.67 (C-γ′), 68.83 (C-β), 68.60 (C-α), 69.57 (C-β′), 68.38 (C-α′).

The ^{1}H NMR spectra of compounds **4a** and **5a** are shown in Figures S1 and S2 (ESI). The ^{1}H, ^{13}C, and ^{1}H–^{13}C HSQC NMR spectra of dyes **1a**,**b** are presented in Figures S3–S10 (ESI).

Spectrophotometric Titration (SPT)

Experiments were conducted in MeCN in 1 and 4.75 cm quartz cells with ground-in stoppers. In each SPT experiment, the total ligand concentration (C_L) was maintained to be constant, and the total concentration of metal perchlorate (C_M) was varied incrementally from 0 up to 6 mM. The C_M-dependent absorption spectra obtained for each of the ligand–metal systems were subjected to global analysis using the methods described previously.[33] The complexation stoichiometry, the complex stability constants, and the absorption spectra of pure complexes were determined by globally fitting the SPT data to the appropriate complexation model (see the Spectrophotometry section). For those systems, where 2:1 (ligand–metal) complexes were detected, the desired characteristics were obtained by globally fitting the SPT data from two experiments conducted at different C_L values in 1 and 4.75 cm cells. When needed, a possible systematic error in the C_M/C_L ratio was taken into account by introducing one more variable parameter into the fitting procedure (in addition to the stability constants).[33] The standard deviations in the stability constants as the fitting parameters did not exceed 1 %.

Density Functional Theory (DFT) Calculations

DFT calculations of 2:1 dye–Ba^{2+} complexes were performed using the Gaussian 09 program package.[34] Geometry optimizations were carried out using the B3LYP functional[35] with the D3(BJ) dispersion correction,[36,37] the 6–31G(d) basis set for H, C, N, O and F, and the SDD basis set for Ba with the corresponding effective core potential (ECP), as implemented in Gaussian 09. The conductor-like polarizable continuum model (CPCM)[38] with the atomic radii optimized for the COSMO-RS method[39] was used to simulate effects of MeCN as the experimental solvent.

For each complex, a set of principal conformations was first calculated in the presence of the continuum solvent field. A few conformers with the lowest DFT/CPCM energies were selected to estimate the Gibbs free energies in solution (G_{soln}). Because G_{soln} is normally calculated on the gas phase geometries,[40] the selected conformers were re-optimized accordingly. All geometry optimizations were followed by frequency calculations to verify the nature of stationary points and to compute thermochemical quantities. The thermochemical analysis was carried out using a scale factor of 0.977 for harmonic frequencies.[41] The G_{soln} values were calculated as follows:

$$G_{soln} = E_{gas} + \Delta G_{corr\_gas} + \Delta G_{solv},$$

where E_{gas} is the electronic energy of the conformer in the gas phase; ΔG_{corr_gas} is the thermal correction to the free energy of the conformer in the gas phase, including the zero point vibrational energy; ΔG_{solv} is the solvation free energy calculated as the difference in electronic energy of the conformer in the presence and absence of the continuum solvent field. The ΔG_{corr_gas} and ΔG_{solv} values were calculated at the same level of theory as that used for the geometry optimizations, whereas the E_{gas} values were derived from the single-point B3LYP-D3(BJ) calculations with the larger def2-TZVP basis set (with the corresponding ECP for Ba).

The structures optimized in the presence of the continuum solvent field were used to calculate π-stacking parameters.

Results and Discussion

Synthesis

1,2-Dichloroanthraqinone (**4a**, Scheme 1) was obtained in two stages from commercially available 2-aminoanthraquinone (**2**). First, compound **3** was prepared by electrophilic chlorination of **2** in position 1 using the known procedure.[31] Then, anthraquinone **3** was diazotized and the diaza group was replaced with a chlorine atom in the presence of CuCl by the Sandmeyer reaction.

1,2- and 1,4-Diphenoxyanthraquinones (**5a**,**b**, Scheme 2) were obtained by nucleophilic substitution of the chlorine atoms in the corresponding dichloroanthraqinones **4a**,**b** by phenoxy groups using the general procedure described in literature.[42]

The crown-containing anthraquinoneimines **1a**,**b** were synthesized photochemically according to the general procedure reported previously,[43] using diphenoxyanthraquinones **5a**,**b** as the starting compounds. In the diphenoxyanthraquinones, one of the phenyl groups is capable of migrating to the *peri*-located oxygen atom under exposure to sunlight, which leads to the formation of 9-phenoxy-1,10-anthraquinone derivatives **6a**,**b** (Scheme 3). The latter have a high reactivity toward nucleophilic agents,[44] which provides easy replacement of the 9-phenoxy group with an arylamino group at room temperature.[45] Compounds **1a**,**b** were prepared using 4′-aminobenzo-15-crown-5 (**7**) as the nucleophilic agent.

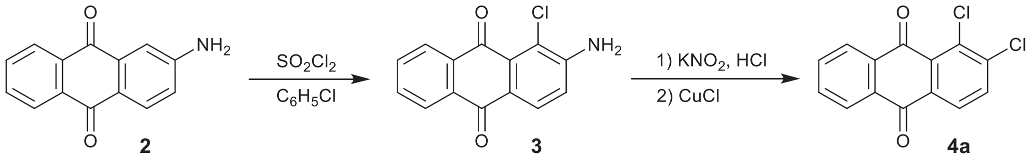

Scheme 1. Synthesis of 1,2-dichloroanthraquinone.

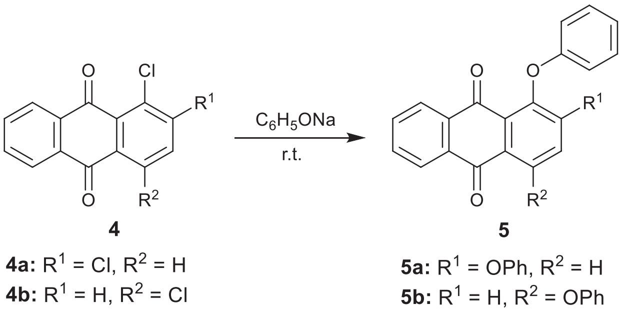

Scheme 2. Synthesis of diphenoxyanthraquinones.

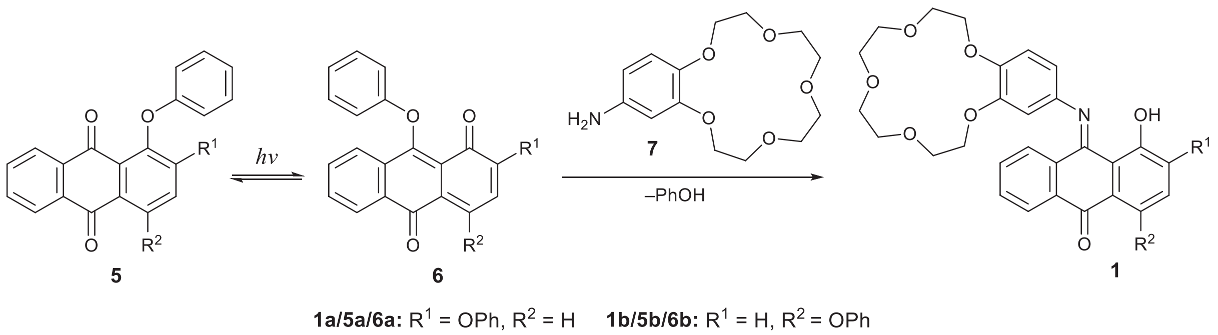

Scheme 3. Synthesis of crown-containing anthraquinoneimines.

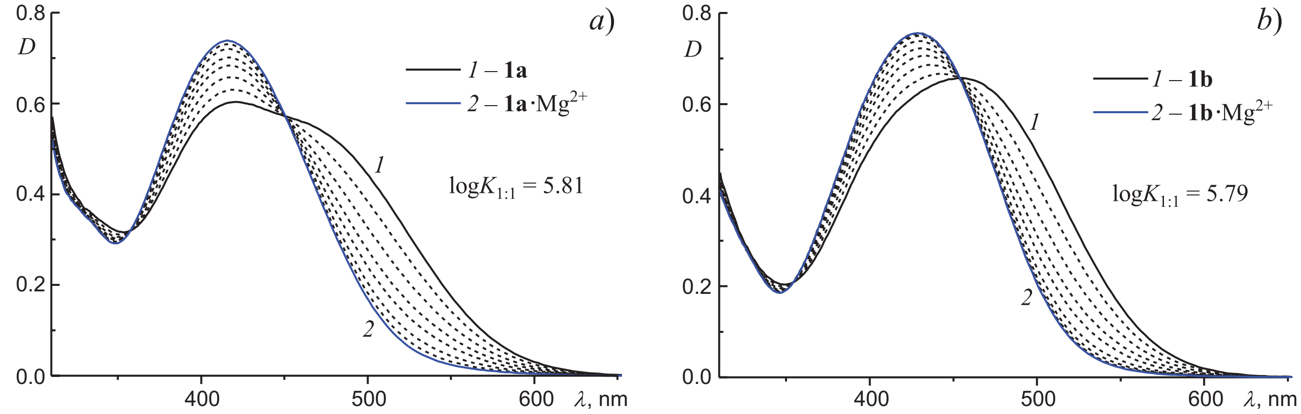

Figure 1. Spectrophotometric titration data for the systems (*a*) **1a**–$Mg(ClO_4)_2$ and (*b*) **1b**–$Mg(ClO_4)_2$ in MeCN (4.75 cm cell; the total ligand concentration is $1.8\cdot10^{-5}$ M; the total metal concentration varies incrementally from 0 to $2.6\cdot10^{-4}$ M).

Spectrophotometry

The complexation of crown-containing dyes **1a**,**b** with alkaline-earth metal perchlorates in MeCN was studied by spectrophotometric titration (SPT, see the Experimental section). The SPT data for the systems **1a**–$Mg(ClO_4)_2$ and **1b**–$Mg(ClO_4)_2$ are presented in Figure 1. The absorption spectra of free dyes **1a** and **1b** in the long-wavelength region (λ = 360–600 nm) are superpositions of two broad overlapping bands. It is known that some imine derivatives of 1-hydroxyanthraquinone can undergo prototropic tautomerization (Scheme 4) and exist as an equilibrated mixture of the imine and enamine isomers both in solution and in the solid state.[45,46] Thus, the double-band absorption profiles of dyes **1a**,**b** could be explained by a coexistence of the imine and enamine tautomers. Provided that this assumption is true, the complexation-induced changes in the spectra of **1a**,**b** can be attributed to a shift of the tautomeric equilibrium towards the imine isomer.[25,26,47] The theoretical rationale for this shift upon 1:1 complexation has been previously reported for a benzo-18-crown-6 ether analog of dye **1d**.[47]

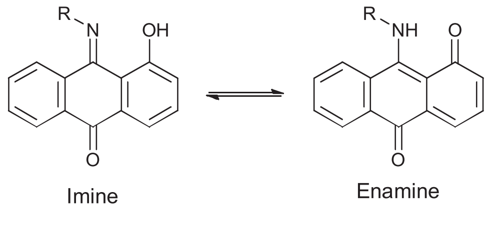

Scheme 4. Prototropic tautomerism of 1-hydroxyanthraquinone-9-imines.

As an alternative, one can assumed that the double-band absorption of **1a**,**b** is due to two different charge-transfer electronic transitions in the imine isomer: the S_0-S_1 transition involves charge transfer from the electron-donating benzocrown moiety to the electron-withdrawing anthraquinoneimine core, and the S_0-S_2 transition leads to a charge redistribution within the asymmetrical anthraquinoneimine core, involving the hydroxy and phenoxy groups. Then, the complexation-induced changes in the absorption spectra of **1a**,**b** can be attributed to hypsochromic shifts of the S_0-S_1 bands of these dyes due to a decrease in the electron-donating strength of the benzocrown moiety upon binding of the metal cation. Note that negative ionochromic effects are typical to the donor–acceptor chromoionophores in which the ionophore is connected with the electron-donating moiety of the chromophore.[48]

The stability constants and absorption spectra of complexes of dyes **1a**,**b** with alkaline-earth metal cations were derived from SPT data using the global analysis methods reported previously.[33] The main results are presented in Table 1. In the case of magnesium and calcium perchlorates, the SPT data were described very well by one equilibrium reaction:

$$\mathrm{L} + \mathrm{M}^{n+} \overset{K_{1:1}}{\rightleftharpoons} \mathrm{L}\cdot\mathrm{M}^{n+}, \tag{1}$$

where L is the dye, M^{n+} is the metal ion, and $K_{1:1} = [L\cdot M^{n+}]/([L][M^{n+}])$ is the stability constant of the 1:1 complex. In the case of strontium and barium perchlorates, the best approximations of SPT data were achieved using two equilibria, namely, equilibrium (1) and the equilibrium involving a 2:1 ligand–metal complex:

$$\mathrm{L}\cdot\mathrm{M}^{n+} + \mathrm{L} \overset{K_{2:1}}{\rightleftharpoons} \mathrm{L}_2\cdot\mathrm{M}^{n+}, \tag{2}$$

where $K_{2:1} = [L_2\cdot M^{n+}]/([L][L\cdot M^{n+}])$ is the stability constant of the 2:1 ligand–metal complex.

Figure 2 allows one to compare the absorption spectra of dye **1a** and complexes **1a**·Ba^{2+} and (**1a**)$_2$·Ba^{2+}. The corresponding data for **1a** with Sr^{2+} and for **1b** with Sr^{2+} and Ba^{2+} are presented in Figures S11–S13 (ESI). In each case, the spectrum of the 2:1 ligand–metal complex is very similar in shape and only slightly different in peak position and intensity from that of the corresponding 1:1 complex. In contrast, the absorption spectra of the related 2:1 and 1:1 complexes of dye **1d**, as reported previously,[25] differ significantly from each other; this was explained by a coexistence of the imine and enamine isomers in MeCN. The enamine form of **1d** is stabilized owing to hydrogen bonding between

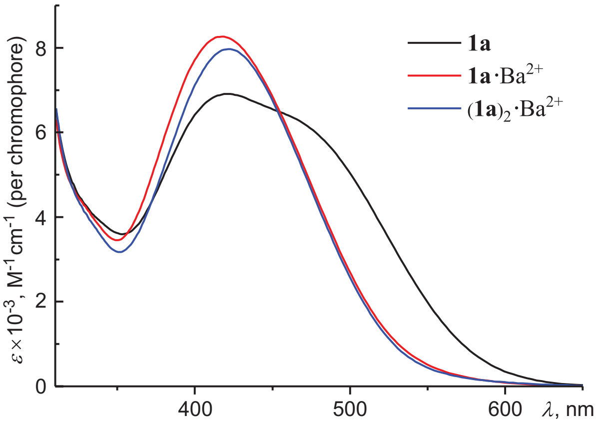

Figure 2. Absorption spectra of dye **1a** and its barium complexes in MeCN.

Table 1. Stability constants and spectrophotometric characteristics of complexes of dyes **1a**,**b** with alkaline-earth metal cations in MeCN.[a]

	log*K*	λ_{max}	$\varepsilon_{max} \cdot 10^{-3}$	$\Delta\lambda$
1a		422	6.92	
1a$\cdot Mg^{2+}$	5.81	416	8.47	–6
1a$\cdot Ca^{2+}$	5.53	416	8.48	–6
1a$\cdot Sr^{2+}$	5.20	417	8.38	–5
(**1a**)$_2\cdot Sr^{2+}$	5.63	423	7.96	+1
1a$\cdot Ba^{2+}$	5.04	417	8.26	–5
(**1a**)$_2\cdot Ba^{2+}$	5.47	422	7.97	0
1b		456	7.93	
1b$\cdot Mg^{2+}$	5.79	429	9.11	–27
1b$\cdot Ca^{2+}$	5.46	429	9.12	–27
1b$\cdot Sr^{2+}$	5.34	430	9.09	–26
(**1b**)$_2\cdot Sr^{2+}$	5.73	433	8.75	–23
1b$\cdot Ba^{2+}$	5.00	432	9.03	–24
(**1b**)$_2\cdot Ba^{2+}$	5.42	433	8.75	–23

[a] K (M^{-1}) = $K_{1:1}$ for $L\cdot M^{n+}$ complexes, $K = K_{2:1}$ for $(L)_2\cdot M^{n+}$ complexes; the K values are determined to within about ±20 %; λ_{max} is the position of the long-wavelength absorption maximum, nm; ε_{max} is the molar absorptivity (per chromophore) at λ_{max}, $M^{-1}cm^{-1}$; $\Delta\lambda = \lambda_{max}(complex) - \lambda_{max}(ligand)$.

the amine hydrogen atom of the benzoylamino group and the nearest oxygen atom of the 1,10-anthraquinone residue. We suppose that dyes **1a**,**b**, in contrast to **1d**, exist in MeCN exclusively as the imine isomers, and the formation of both 2:1 and 1:1 complexes leads to an increase in the S_0-S_1 transition energy, so that the S_0-S_1 and S_0-S_2 transitions become close in energy (see the above hypothesis about two different charge-transfer electronic transitions in anthraquinoneimines **1a**,**b**).

Figure 3 demonstrates that for dyes **1a**,**b** with alkaline-earth metal cations the stability constant of the 1:1 complex decreases monotonically as the cation radius increases (see also Table 1). Similar dependencies have been observed for benzo-15-crown-5 (B15C5) and dyes **1c**,**d**.[25] Compounds **1a**–**d**, as compared with B15C5, are characterized by lower $K_{1:1}$ values due to the electron-withdrawing influence of the anthraquinone residue on the benzocrown moiety. It is noteworthy that the 2:1 complexes of dyes **1a**,**b** with Sr^{2+} and Ba^{2+} have higher stability constants than the corresponding 1:1 complexes (see Figure 3 and Table 1).

Table 2 shows the ratios of the stability constants of the 2:1 and 1:1 ligand–metal complexes, $K_{2:1}/K_{1:1}$, for B15C5 and dyes **1a–d** with Sr^{2+} and Ba^{2+}. The pronounced differences in $K_{2:1}/K_{1:1}$ between B15C5 ($K_{2:1}/K_{1:1} < 1$) and dyes **1a**–**d** ($K_{2:1}/K_{1:1} > 1$) are explained by additional π-stacking interactions in the sandwich complexes of the dyes.[25] The fact that the $K_{2:1}/K_{1:1}$ ratios with both Sr^{2+} and Ba^{2+} increase significantly on changing from dye **1c** to its 2-benzoylamino-substituted analog **1d** was attributed to a larger number of short stacking contacts (4 *vs.* 2) in the sandwich complexes formed by **1d**.[25] The $K_{2:1}/K_{1:1}$ values measured for dyes **1a**,**b** are very close to the corresponding values measured for **1c**. This suggests that additional stacking contacts involving phenyl rings in the sandwich complexes formed by the phenoxy derivatives of **1c** are very weak.

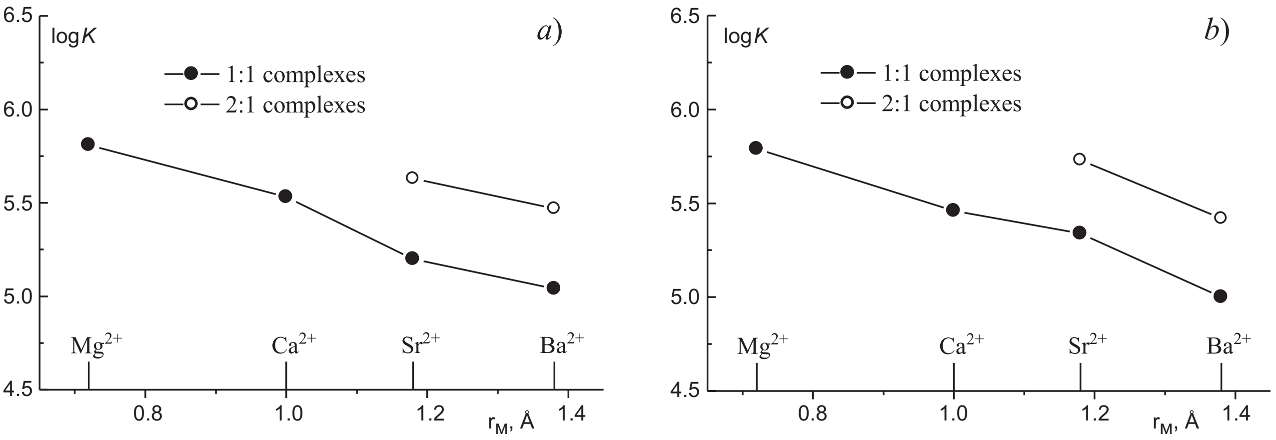

Figure 3. Plots of log*K* *vs.* the metal cation radius (r_M) for the 1:1 and 2:1 complexes of dyes (*a*) **1a** and (*b*) **1b** with alkaline-earth metal cations in MeCN; the r_M values are taken from ref.[49]

Table 2. Ratios of the stability constants of the 2:1 and 1:1 ligand–metal complexes for dyes **1a–d** and B15C5 with the Sr^{2+} and Ba^{2+} ions in MeCN.[a]

Ligand	B15C5	**1a**	**1b**	**1c**	**1d**
$K_{2:1}/K_{1:1}$ (Sr^{2+})	0.35	2.68	2.46	1.01	8.75
$K_{2:1}/K_{1:1}$ (Ba^{2+})	0.67	2.70	2.72	2.26	7.60

[a] The $K_{2:1}/K_{1:1}$ ratios for B15C5 and dyes **1c**,**d** are taken from ref.[25]

Molecular Structure Calculations

The molecular structures of complexes $(\mathbf{1a},\mathbf{b})_2\cdot Ba^{2+}$ in MeCN were studied by DFT calculations (computational details are given in the Experimental section; Cartesian coordinates and energies for calculated structures are presented in Tables S1–S6, ESI). Figure 4 shows the most stable conformers of complexes $(\mathbf{1a},\mathbf{b},\mathbf{d})_2\cdot Ba^{2+}$. The structure of $(\mathbf{1d})_2\cdot Ba^{2+}$ was calculated previously by the same method.[29] In all three structures, the benzocrown moieties adopt an *s-trans* conformation with respect to the imine double bond, the 1-hydroxyanthraquinone residues are in an *anti* orientation relative to each other, and the non-planar anthraquinone cores face each other with the convex sides. To denote conformations with convex and concave arrangements of the anthraquinone cores, we used prefixes "*in*" and "*out*", respectively. The *in*-[*anti*-(*s-trans*)$_2$] conformers of complexes $(\mathbf{1a},\mathbf{b},\mathbf{d})_2\cdot Ba^{2+}$ were calculated to be 0.5–1.1 kcal/mol more stable than the corresponding *out* conformers.

Table S7 (ESI) shows some geometrical parameters of the stacking contacts between aromatic rings in complexes $(\mathbf{1a}–\mathbf{d})_2\cdot Ba^{2+}$. The aromatic rings common to compounds **1a**–**d** are denoted in the Introduction section by symbols **A**, **C**, and **D**. Complexes $(\mathbf{1a})_2\cdot Ba^{2+}$ and $(\mathbf{1d})_2\cdot Ba^{2+}$ are characterized by the same number (four) of stacking contacts. In complex $(\mathbf{1a})_2\cdot Ba^{2+}$, there are two edge-to-face contacts between the phenyl ring (**Ph**) of one molecule and the ring **A** of the other. In complex $(\mathbf{1d})_2\cdot Ba^{2+}$, the benzoyl rings (**Bz**) contact with the rings **A** approximately in a face-to-face manner. There are no critical differences between these complexes in parameters of the **C**···**C** and **D**···**D** contacts. The fact that the experimental $K_{2:1}/K_{1:1}$ ratio for $(\mathbf{1a})_2\cdot Ba^{2+}$ is almost three times lower than that for $(\mathbf{1d})_2\cdot Ba^{2+}$ and very close to that for $(\mathbf{1c})_2\cdot Ba^{2+}$ (Table 2) suggests that the edge-to-face **Ph**···**A** contacts in $(\mathbf{1a})_2\cdot Ba^{2+}$ are very weak. Note that face-to-face contacts between **Ph** and **A** are impossible in the $(\mathbf{1a})_2\cdot Ba^{2+}$ complex due to steric repulsion between the phenyl and hydroxyl groups.

Complex $(\mathbf{1b})_2\cdot Ba^{2+}$ has three stacking contacts: **C**···**C**, **D**···**D**, and **Ph**···**Ph**. The latter is characterized by relatively long stacking distance (3.62 Å), the angle between the planes of the phenyl rings being about 32°. In this complex, a phenyl hydrogen atom of one molecule forms a weak hydrogen bond (2.25 Å in length) with the carbonyl oxygen atom of the other (in total, two hydrogen bonds are formed).

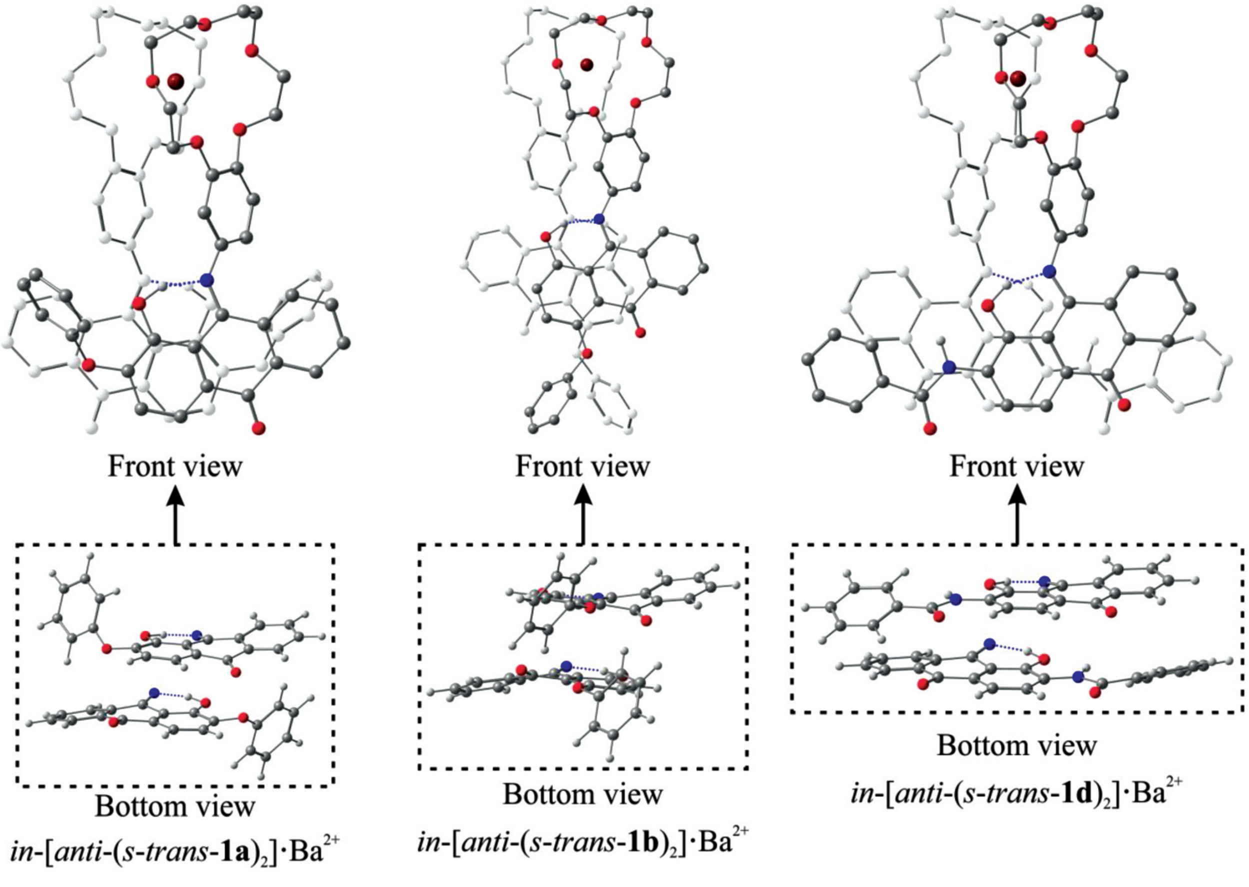

Figure 4. Most stable conformations of complexes $(\mathbf{1a},\mathbf{b},\mathbf{d})_2\cdot Ba^{2+}$ in MeCN, as derived from DFT calculations; hydrogen atoms, except the hydroxyl ones, are not shown in the front view; benzocrown moieties are not shown in the bottom view.

The formation of hydrogen bonds leads to an increased displacement between the rings **C** and, most probably, to a weakening of the **C**···**C** contact, so that the hydrogen bonding ultimately has insignificant effect on the $K_{2:1}/K_{1:1}$ ratio (compare data for dyes **1b** and **1c** in Table 2).

Conclusions

The crown-containing 1-hydroxy-9,10-anthraquinone-9-imines **1a**,**b** were obtained photochemically from 1,2(4)-diphenoxyanthraquinones and 4′-aminobenzo-15-crown-5. In MeCN, the absorption spectra of dyes **1a**,**b** in the long-wavelength region (λ = 360–600 nm) are superpositions of two broad overlapping bands. The double-band absorption can be explained either by the imine–enamine tautomerization in this solvent or by the existence of two different charge-transfer electronic transitions in the imine form: the S_0-S_1 transition involves charge transfer from the electron-donating benzocrown moiety to the electron-withdrawing anthraquinoneimine core, and the S_0-S_2 transition leads to a charge redistribution within the asymmetrical anthraquinoneimine core, involving the hydroxy and phenoxy groups. The second assumption is better consistent with the changes in the absorption spectra observed upon the complexation of dyes **1a**,**b** with alkaline-earth metal cations. Compounds **1a**,**b** are capable of binding the Sr^{2+} and Ba^{2+} ions to form 2:1 (ligand–metal) sandwich-type complexes that exhibit higher stability constants than the corresponding 1:1 complexes. The $K_{2:1}/K_{1:1}$ values measured for dyes **1a**,**b** with Sr^{2+} and Ba^{2+} are very close to the corresponding values measured for the analogous dye lacking phenoxy groups (compound **1c**). This suggests that additional stacking contacts involving phenyl rings in the sandwich complexes formed by dyes **1a**,**b** are very weak.

Acknowledgements. This work was supported by the Russian Foundation for Basis Research with respect to the synthesis and spectroscopic studies [project No. 18-43-860005] and by the Ministry of Science and Higher Education of the Russian Federation with respect to the quantum-chemical calculations [State Assignment No. 0089-2019-0003]. The work was performed using the equipment of the Multi-User Analytical Center of IPCP RAS.

Disclosure statement. No potential conflict of interest was reported by the authors.

References

1. Meyer E.A., Castellano R.K., Diederich F. *Angew. Chem. Int. Ed.* **2003**, *42*, 1210–1250.
2. Burley S.K., Petsko G.A. *Science* **1985**, *229*(4708), 23–28.
3. Bhattacharyya R., Samanta U., Chakrabarti P. *Protein Eng. Des. Sel.* **2002**, *15*, 91–100.
4. Kannan N., Vishveshwara S. *Protein Eng. Des. Sel.* **2000**, *13*, 753–761.
5. Wheeler S.E. *Acc. Chem. Res.* **2013**, *46*, 1029–1038.
6. Hunter C.A., Lawson K.R., Perkins J., Urch C.J. *J. Chem. Soc., Perkin Trans. 2* **2001**, *5*, 651–669.
7. Chen T., Li M., Liu J. *Cryst. Growth Des.* **2018**, *18*, 2765–2783.
8. Kumar S. *Liq. Cryst.* **2004**, *31*, 1037–1059.
9. Cui Z.-h., Lischka H., Beneberu H.Z., Kertesz M. *J. Am. Chem. Soc.* **2014**, *136*, 12958–12965.
10. Pedersen C.J. *J. Am. Chem. Soc.* **1970**, *92*, 386–391.
11. An H., Bradshaw J.S., Izatt R.M., Yan Z. *Chem. Rev.* **1994**, *94*, 939–991.
12. Liu Z., Luo F., Ju X.-J., Xie R., Luo T., Sun Y.-M., Chu L.-Y. *Adv. Funct. Mater.* **2012**, *22*, 4742–4750.
13. Yu H.-R., Hu J.-Q., Lu X.-H., Ju X.-J., Liu Z., Xie R., Wang W., Chu L.-Y. *J. Phys. Chem. B* **2015**, *119*, 1696–1705.
14. Wu H.-G., Ju X.-J., Xie R., Liu Y.-M., Deng J.-G., Niu C.H., Chu L.-Y. *Polym. Adv. Technol.* **2011**, *22*, 1389–1394.
15. Park J., Kim K.Y., Kim C., Lee J.H., Kim J.H., Lee S.S., Choi Y., Jung J.H. *Polym. Chem.* **2018**, *9*, 3900–3907.
16. Yu H.-R., Ju X.-J., Xie R., Wang W., Zhang B., Chu L.-Y. *Anal. Chem.* **2013**, *85*, 6477–6484.
17. Gromov S.P., Fedorova O.A., Ushakov E.N., Buevich A.V., Baskin I.I., Pershina Yu.V., Eliasson B., Edlund U., Alfimov M.V. *J. Chem. Soc., Perkin Trans. 2* **1999**, *7*, 1323–1330.
18. Gromov S.P., Vedernikov A.I., Fedorov Yu.V., Fedorova O.A., Andryukhina E.N., Shepel’ N.E., Strelenko Yu.A., Johnels D., Edlund U., Saltiel J., Alfimov M.V. *Russ. Chem. Bull.* **2005**, *54*, 1569–1579.
19. Gromov S.P., Vedernikov A.I., Lobova N.A., Kuz’mina L.G., Basok S.S., Strelenko Yu.A., Alfimov M.V., Howard J.A.K. *New J. Chem.* **2011**, *35*, 724–737.
20. Koçoğlu S., Ogutcu H., Hayvalı Z. *Res. Chem. Intermed.* **2019**, *45*, 2403–2427.
21. Lin S.-Y., Liu S.-W., Lin C.-M., Chen C.-h. *Anal. Chem.* **2002**, *74*, 330–335.
22. Ho M.-L., Hsieh J.-M., Lai C.-W., Peng H.-C., Kang C.-C., Wu I-C., Lai C.-H., Chen Y.-C., Chou P.-T. *J. Phys. Chem. C* **2009**, *113*, 1686–1693.
23. Sherman C.L., Brodbelt J.S., Marchand A.P., Poola B. *J. Am. Soc. Mass Spectrom.* **2005**, *16*, 1162–1171.
24. Frański R., Gierczyk B. *J. Am. Soc. Mass Spectrom.* **2010**, *21*, 545–549.
25. Martyanov T.P., Klimenko L.S., Kozlovskiy V.I., Ushakov E.N. *Tetrahedron* **2017**, *73*, 681–691.
26. Martyanov T.P., Ushakov E.N., Klimenko L.S. *Macroheterocycles* **2013**, *6*, 240–244.
27. Watt M., Hardebeck L.K.E., Kirkpatrick C.C., Lewis M. *J. Am. Chem. Soc.* **2011**, *133*, 3854–3862.
28. Sherrill C.D. *Acc. Chem. Res.* **2013**, *46*, 1020–1028.
29. Martyanov T.P., Kudrevatykh A.A., Strelnikov I.G., Klimenko L.S., Korchagin D.V., Chernyak A.V., Ushakov E.N. *Supramol. Chem.* **2018**, *30*, 918–928.
30. Gottlieb H.E., Kotlyar V., Nudelman A. *J. Org. Chem.* **1997**, *62*, 7512–7515.
31. Gudzenko V.I., Leichenko L.D. USSR Pat. **1974**, No. 436819.
32. Mart’yanov T.P., Klimenko L.S., Ushakov E.N. *Russ. J. Org. Chem.* **2016**, *52*, 1126–1136.
33. Ushakov E.N., Gromov S.P., Fedorova O.A., Pershina Yu.V., Alfimov M.V., Barigilletti F., Flamigni L., Balzani V. *J. Phys. Chem. A* **1999**, *103*, 11188–11193.
34. *Gaussian 09, Revision E.01.* Gaussian, Inc., Wallingford CT, **2013**.
35. Becke A.D. *J. Chem. Phys.* **1993**, *98*, 5648–5652.
36. Grimme S., Antony J., Ehrlich S., Krieg H. *J. Chem. Phys.* **2010**, *132*, 154104.
37. Grimme S., Ehrlich S., Goerigk L. *J. Comput. Chem.* **2011**, *32*, 1456–1465.
38. Cossi M., Rega N., Scalmani G., Barone V. *J. Comp. Chem.* **2003**, *24*, 669–681.
39. Klamt A., Jonas V., Bürger T., Lohrenz J.C.W. *J. Phys. Chem. A* **1998**, *102*, 5074–5085.

40. Ho J., Klamt A., Coote M.L. *J. Phys. Chem. A* **2010**, *114*, 13442–13444.
41. Alecu I.M., Zheng J., Zhao Y., Truhlar D.G. *J. Chem. Theory Comput.* **2010**, *6*, 2872–2887.
42. Kudrevatykh A.A., Neznaeva D.A., Martyanov T.P., Klimenko L.S. *Russ. Chem. Bull.* **2019**, *68*, 623–627.
43. Klimenko L.S., Kusov S.Z., Vlasov V.M. *Mendeleev Commun.* **2002**, *12*, 102–103.
44. Gritsan N.P., Klimenko L.S. *J. Photochem. Photobiol. A* **1993**, *70*, 103–117.
45. Gritsan N.P., Klimenko L.S., Leonenko Z.V., Mainagashev I.Ya., Mamatyuk V.I., Vetchinov V.P. *Tetrahedron* **1995**, *51*, 3061–3076.
46. Yatsenko A.V., Tafeenko V.A., Zhukov S.G., Medvedev S.V., Popov S.I. *Struct. Chem.* **1997**, *8*, 197–204.
47. Martyanov T.P., Ushakov E.N., Savelyev V.A., Klimenko L.S. *Russ. Chem. Bull.* **2012**, *61*, 2282–2294.
48. Ushakov E.N., Alfimov M.V., Gromov S.P. *Macroheterocycles* **2010**, *3*, 189–200.
49. Shannon R.D. *Acta Cryst. A* **1976**, *32*, 751–767.

Received 10.02.2020
Accepted 10.03.2020